Implementing unsteady friction in Pressure-Time measurements

PhD Pontus P. Jonnson

Pöyry SwedPower AB, Sweden. pontus.jonsson@poyry.com

PhD Jørgen Ramdal

Gauldal Consult AS, Norway. jorgen.ramdal@gauldalconsult.no

Professor Michel J. Cervantes

Luleå University of Technology, Sweden. michel.cervantes@ltu.se

Professor Torbjørn Kristian Nielsen

Norwegian University of Science and Technology, Norway. torbjorn.nielsen@ntnu.no

Abstract

Laboratory measurements using the pressure-time method showed a velocity or Reynolds number dependent error of the flow estimate. It was suspected that the quasi steady friction formulation of the method was the cause. This was investigated, and it was proved that implementing a model for unsteady friction into the calculations improved the result. This paper presents the process of this investigation, and proposes a new method for treatment of the friction term in the pressure-time method.

Key words: Gibson method, Pressure-Time, Unsteady friction

Introduction

NTNU and LTU collaborated on the development of the pressure-time method, also known as the Gibson method, through the PhD-projects of Pontus Jonsson[3] and Jørgen Ramdal [4]. The Gibson method is commonly used for measuring flow in closed conduits. It is based on Newton's second law. The retardation of the water during a valve closure generates a pressure force in the conduit. The differential pressure between two cross-sections is measured during the deceleration, and the discharge is then calculated by integrating the differential pressure over time [1,2];

$$Q = \frac{A}{\rho L} \int_0^t (\Delta P + \xi)\, dt + \text{q}. \tag{1}$$

where Q is the discharge, A is the cross-sectional area, L is the distance between the cross sections, ρ is the water density, ΔP is the differential pressure, ξ is the pressure loss due to friction, t is the time and q is the leakage flow after the closure. Figure 1 shows an example of a Gibson's calculation.

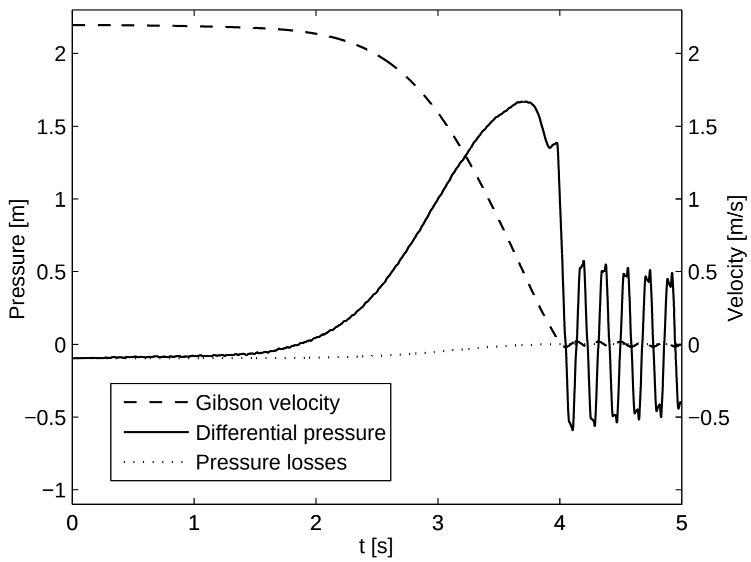

Figure 1: Example of a Gibson's integrated velocity with corresponding differential pressure and pressure losses. Data obtained from a simulated valve closure using a 1-dimensional model ($Re=0.65\cdot10^6$, D=0.3 m), Jonsson [3].

For this article the treatment of the friction, ξ, is the main issue, and the other elements of the Gibson method are not further explained. Previous work with laboratory measurements and numerical simulations performed by Jonsson *et al.* [1] led to an overestimation and an underestimation of the calculated flow rate. It indicated that the assumption of a constant friction factor may not be appropriate. The Gibson method uses a quasi-steady state assumption for the pressure loss calculation during the closure, i.e., the pressure losses are calculated at each time step, assuming a steady state. Furthermore, the friction factor, obtained from the initial flow, is assumed constant throughout the closure. This type of assumption is only valid for a rough pipe and a very slow closure. However, the effect of unsteadiness may be significant on the losses [5] and should therefore be included in the Gibson method, the object of the present paper.

Unsteady friction

Friction for decelerating flows is a topic that has been, and still is, subjected to research. Shuy [6] and Kurokawa and Morikawa [7] found that the unsteady wall shear stress was greater than the quasi-steady shear stress in decelerated flows. However, Ariyarante *et al.* [8] showed that the unsteady wall friction can either under-shoot or over-shoot the quasi-steady friction, depending on the flow conditions. Key features of decelerating flow may be described by the non-dimensionless parameter δ according to Ariyarante et al. [8]:

$$\delta = \frac{v}{u_{\tau_0}^2}\left(\frac{1}{U_0}\frac{dU}{dt}\right) \tag{2}$$

$v/(u^2_{\tau 0})$ represents the viscous time scale and $U_0/(dU/dt)$ represents the time scale related to the acceleration. As δ increases, the effects of viscosity will be more pronounced and the profile will be similar to a quasi-steady profile. On the other hand, for small values of δ, the effects of viscosity will be confined near the wall and most of the flow will act like a plug flow. More information on the subject may be found in [8].

Numerical investigation

A quantification of the different physical quantities involved in the Gibson method was performed with the help of numerical simulation. In previous stages of the project, Jonsson [3] had developed a numerical model that gave good agreement between simulated and laboratory measurements on the method. The geometry, valve characteristics, flows and pipe roughness used in the laboratory measurements were used as boundary conditions for the simulations. The specifications for the laboratory measurements are found in Table 1, and a schematic of the test rig is presented in Figure 2. More detailed specifications for the laboratory measurements can be found in Jonsson *et al.* [1].

Table 1: Specifications of the NTNU test rig.

Pipe diameter	0.3 m	
Measurement cross section distances	3–21 m (For this paper 6 and 9 m are evaluated)	
Pressure	9.75 m w.c*	
Valve closure time	~5 s	
Investigated flow rates	~0.16, ~0.3 and ~0.4 m^3/s	
Corresponding Reynolds number	$\sim 0.65\cdot 10^6$, $\sim 1.25\cdot 10^6$and $\sim 1.70\cdot 10^6$	
Total pipe length	~40 m	

*w.c: water column

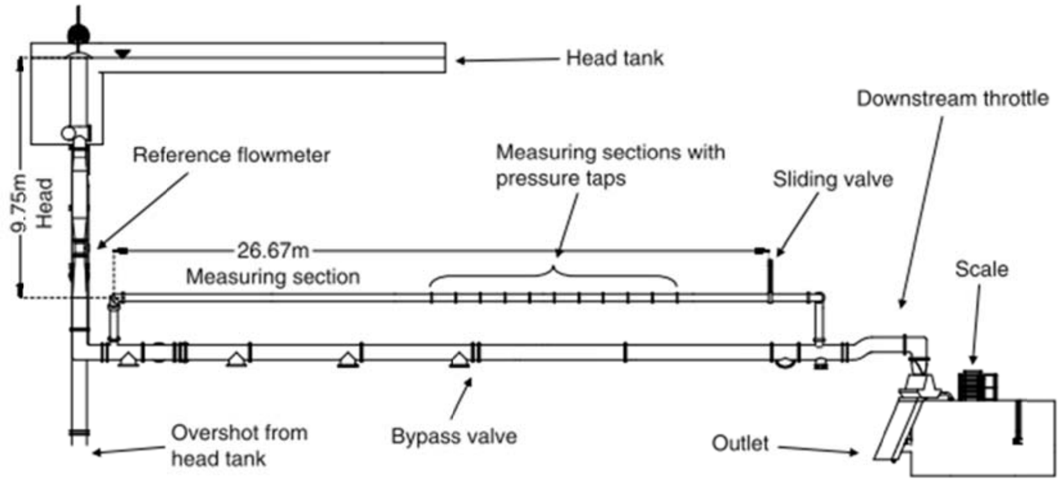

Figure 2: Schematic of the test rig at NTNU.

The numerical method used was Method of Characteristics (MOC), which is the most commonly used method for fast transients. It is a one dimensional method and has the advantage of being fast with regards to computations. A detailed explanation of the method can be found in Wylie and Streeter [10]. There exist some different friction models which are easy to implement in MOC. Among these, and one of the most commonly used, is Brunone's friction model [9]:

$$f = f_q + \frac{kD}{u|u|}\left(\frac{\partial u}{\partial t} - a\frac{\partial u}{\partial x}\right) \tag{3}$$

In this equation f_q is the quasi-steady friction factor, D is pipe diameter, u is the bulk velocity, and *a* is the wave speed. The coefficient *k* is a weighting coefficient for the convective (du/dx) and temporal accelerations (du/dt) introduced in the friction factor. It can be calibrated empirically for certain flows, or another approach is to use Vardy's shear decay coefficient C*, which is related to k by (empirically calibrated [9]):

$$k = \sqrt{C^*}/2 \tag{4}$$

Vardy's shear decay coefficient for laminar flow (Re<2300) is C* = 0.00476. For turbulent flow it is:

$$C^* = \frac{7.41}{Re^{\log\left(14.3/Re^{0.05}\right)}} \tag{5}$$

As explained, the assumption that the quasi steady friction factor can be treated as a constant is only valid for flow in rough pipes with slow decelerations. Therefore, this assumption is rejected and the quasi-steady friction factor, f_q, is instead modeled by Darcy's friction factor in the laminar flow regime (f_q = 64/Re) and Haaland's equation for the turbulent regime;

$$f_q = \left(-1.8 \cdot \log\left(\left(\frac{6.9}{\mathrm{Re}}\right) + \left(\frac{\varepsilon/_D}{3.7}\right)^{1.11}\right)\right)^{-2} \tag{6}$$

The coefficients k and f_q are set to follow the instantaneous Reynolds number, i.e., the coefficients are updated for the local velocity at each grid point and time step. To evaluate the importance of the friction terms in the Brunone model, each term (f_q, du/dt and du/dx) is explicitly added in the MOC and the contribution to the friction from each term can then be studied during the closure event. Figure 3 shows the last part of the closure and the two first subsequent pressure reaches. During the closure, the quasi-steady term contributes, as expected, to the major portion of the positive friction, i.e., friction in the direction of the bulk flow. The temporal term gives most of the negative contribution to the friction, i.e., the term has a negative sign during deceleration of the flow, while the convective term is negligible. After closure, the friction from the temporal term has a 90° phase shift with the bulk velocity, while the friction from the convective term has the same phase as the velocity. The convective acceleration is also found to have a 90° phase shift with the pressure wave. Regarding the Gibson integration, the convective term can be rejected from the further calculations. This is because the integration end point in the Gibson method is near the top of the pressure peaks that follows the closure [2]. The contribution to the integral from the convective term is therefore almost canceled out. This is also convenient since the convective term is difficult to implement in the calculations for a real case.

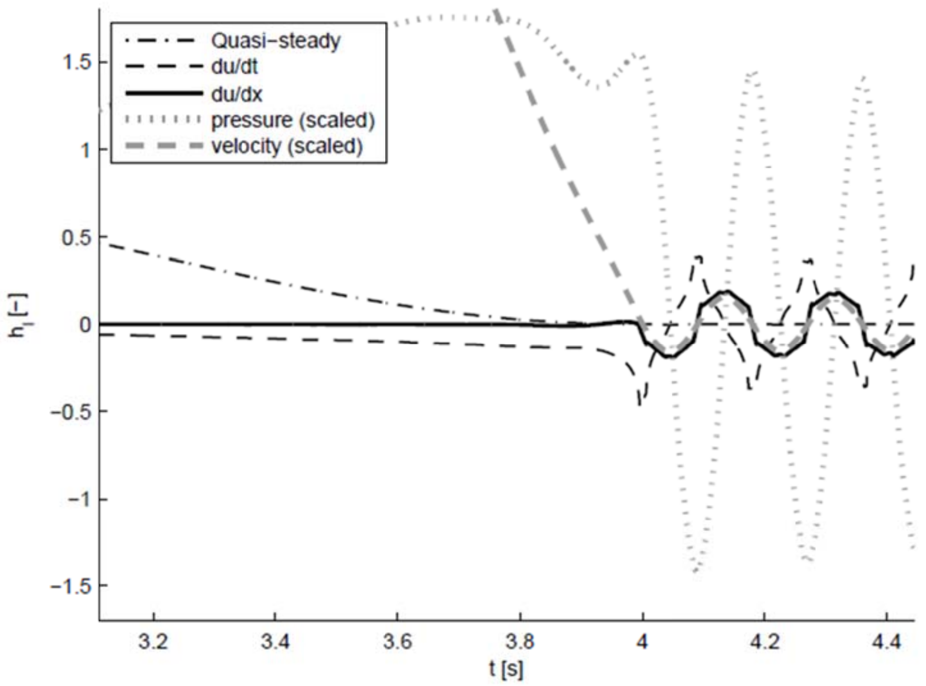

Figure 3: Simulated valve closure, with the differential pressure and velocity together with the friction due to each term in the Brunone model.

New proposed calculation procedure

After the numerical analysis, a modification of the Gibson method, with the addition of unsteady friction, is proposed. The modified method is referred to as "unsteady Gibson" (UG) and the unmodified method as "standard Gibson" (SG). The unsteady friction is implemented in the Gibson method (UG) through a simplified version of the Brunone friction model:

$$f = f_q + \frac{kD}{u|u|}\left(\frac{\partial u}{\partial t}\right) \tag{7}$$

To implement unsteady friction in the calculations, the velocity at each time step (dashed curve in Fig. 1) is needed for the calculation of f_q, Re, k and du/dt. The velocity is found from the following equation:

$$u_i = \frac{Q_0}{A} - \frac{1}{\rho L}\int_0^i (\Delta P_i + \xi_i)dt, \tag{8}$$

where Q_0 is the flow rate found from previous iteration. The flow rate (Q_0) for the first iteration is estimated by assuming a linear pressure loss in time. New pressure losses for each time step are calculated using the unsteady expression of the friction factor, and the relation between the friction factor, f, and the pressure loss, ξ:

$$\xi = f \cdot \left(\frac{L \cdot \rho \cdot u^2}{2 \cdot D}\right) \tag{9}$$

Another parameter that is calculated and inserted into the calculations is the pipe roughness. This is found by inserting initial friction factor and Reynolds number into equation 6. A new Gibson integration can thereafter be performed with the updated pressure losses, and this loop continues until a convergence criterion is satisfied. Figure 4 shows an overview of the procedure.

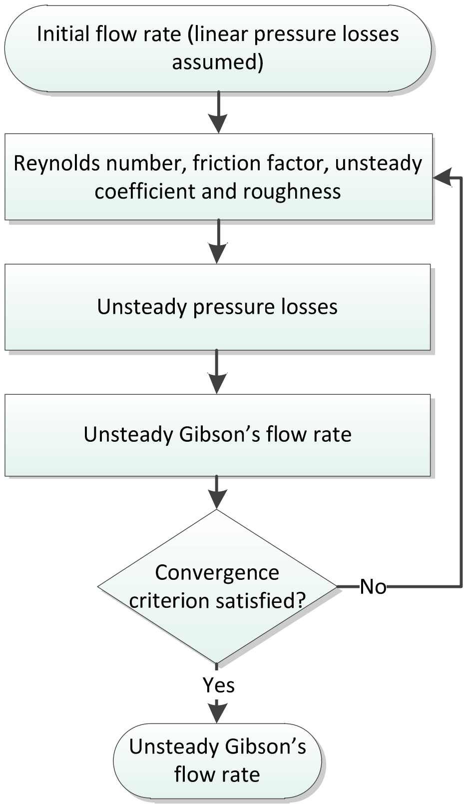

Figure 4: Procedure of unsteady Gibson's calculation.

Results

Comparisons of the Standard Gibson (SG) (IEC 41 [2]) and the Unsteady Gibson (UG) were made with both simulated valve closures and the experiments performed at the NTNU test rig. As mentioned, the simulations were performed with same geometry (simplified), boundary conditions and pipe roughness as in the experiments. The pressure was extracted at the same positions as in the experiments.

Figure 5 shows the flow rate estimation error for SG and UG calculated from a simulated valve closure. It can be seen that for, most points, the estimation from UG is closer to the reference compared to SG. For a test section length of 6 m, UG corrects both the over and underestimation of the SG estimated flow rate.

Figure 6 shows the flow rate estimation error for SG and UG calculated from the experiments (compared to an accurate magnetic flow meter). The experimental results show similar trend as from the simulated, where UG gives an estimate closer to the reference for most of the points. The uncertainty bars (UG) enclose or are close to the zero value for most of the tested points. However, because the bars from both SG and UG overlap each other, the deviation from the mean of the difference was calculated, i.e., the difference between SG and UG at the same closure event. This will reduce the random error between each run and enhance the systematic behavior. Table 2 shows the deviation from the mean of the difference at a 95% confidence level. The deviation is small and, thus, the difference between SG and UG is almost constant for each run.

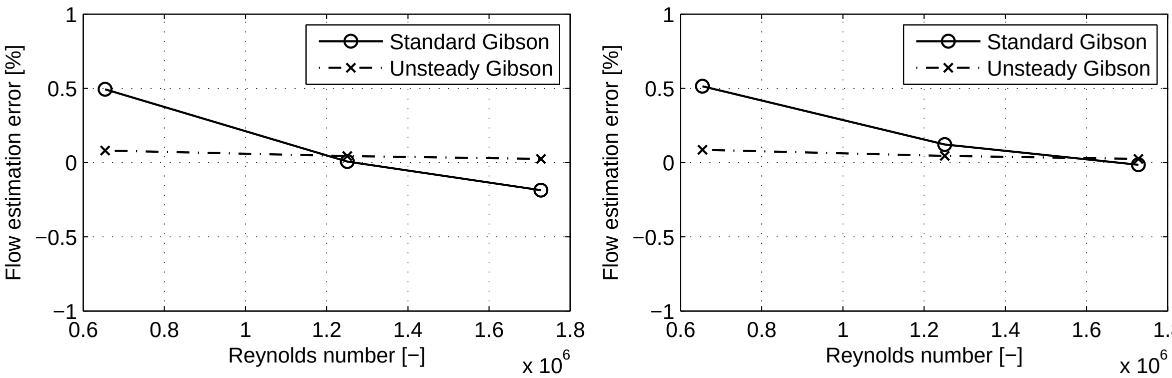

Figure 5: Deviation of the standard and unsteady Gibson-estimated flow rate relative the initial flow from simulations. Left figure corresponds to a test section length of 6 m and right figure to a length of 9 m.

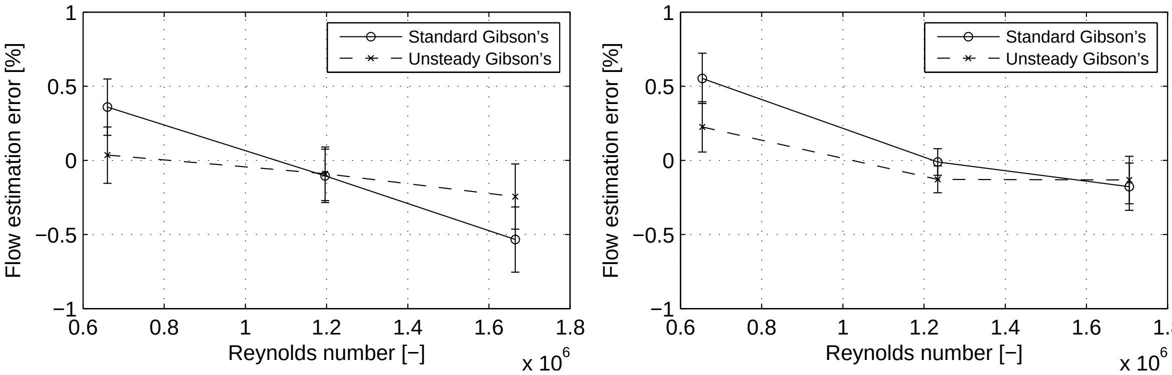

Figure 6: Deviation of the standard and unsteady Gibson-estimated flow rate from the reference. Left figure corresponds to a test section length of 6 m and right figure to a length of 9 m. The bars correspond to the uncertainty of the mean at the 95% confidence level.

Table 2: The difference between the unsteady and standard Gibson estimates, and the uncertainty from the mean of the difference at 95 % confidence level (calculated from 12 runs).

Reynolds number		Re=0.65·10^6	Re= 1.25·10^6	Re=1.70·10^6
6 m distance between measurement cross sections	Difference	0.4 %	0 %	-0.3 %
	Uncertainty	0.01 %	0.02 %	0.06%
9 m distance between measurement cross sections	Difference	0.4 %	0.1 %	-0.05 %
	Uncertainty	0.05 %	0.02 %	0.04 %

Further work

The result in this article is based on one test set up with a quite small diameter of 0.3 m. Validation of the data and method is also needed on site efficiency tests against an accurate reference, in order to find limitations on the method and maybe find a calibration for the influence from unsteady friction at higher Reynolds numbers.

Conclusion

A modification of the Gibson procedure, where a simplified version of Brunone's friction model is implemented in the calculations, has proved to give a more accurate estimation of the flow rate compared to the standard Gibson method procedure. The new procedure corrects both overestimation and underestimation of the flow, and the estimation error was reduced by up to 0.4%. Such improvement can be of great importance for site efficiency tests.

References

[1] Jonsson P. P., Ramdal J. Cervantes M. J., “Experimental Investigation of the Gibson’s Method outside Standards”, Proceedings of the 24th Symposium on Hydraulic Machinery and System, Foz do Iguacu, Brazil, 2008.

[2] IEC., 1991, International Standard – Field acceptance tests to determine the hydraulic performance of hydraulic turbines, storage pumps and pump-turbines. Volume 41, third edition, pp. 146-160, Geneva, Switzerland.

[3] Jonsson P. P., Flow and pressure measurements in low-head hydraulic turbines. PhD thesis, Luleå University of Technology, Sweden, 2011.

[4] Ramdal J., Efficiency measurements in low head hydro power plants. PhD thesis, Norwegian University of Science and Technology, Norway 2011

[5] Cervantes M. J., Gustavsson H. L.. Unsteadiness and viscous losses in hydraulic turbines. J Hydraul Res 2006;44(2):249–58.

[6] Shuy E. B.. Wall shear stress in accelerating and decelerating turbulent pipe flows. J Hydraul Res 1996;34(2):173–83.

[7] Kurokawa J., Morikawa M.. Accelerated and decelerated flows in a circular pipe. JSME 1986;29(249):758–65.

[8] Ariyarante C., He S., Vardy A. E.. Wall friction and turbulence dynamics in decelerating pipe flows. J Hydraul Res 2010;48(6):810–21.

[9] Bergant A., Simpson A. R., Vitkovsky J. Developments in unsteady pipe flow friction modelling. J Hydraul Res 2001;39(3):249–57.

[10] Wylie E., Streeter V. L.. Fluid transients in systems. Upper saddle river (New Jersey, USA): Prentice Hall; 1993.